Dynamics in Multicomponent Polyelectrolyte Solutions

Sanghun Lee,[†] Vijay R. Tirumala,[†,⊥] Michihiro Nagao,[§] Taiki Tominaga,[†,‡] Eric K. Lin,[†] Jian Ping Gong,[‡] and Wen-li Wu*[,†]

Polymers Division, National Institute of Standards and Technology, Gaithersburg, Maryland; Graduate School of Sciences, Hokkaido University, Sapporo Japan; and NIST Center for Neutron Research, National Institute of Standards and Technology, Gaithersburg, Maryland

Received October 2, 2008; Revised Manuscript Received December 19, 2008

ABSTRACT: Double-network hydrogels (DN-gels) prepared from the combination of a moderately cross-linked anionic polyelectrolyte (poly(2-acrylamido-2-methyl-1-propanesulfonic acid), PAMPS) and an un-cross-linked linear polymer (polyacrylamide, PAAm) solution show strong mechanical properties far superior to that of their individual constituents. To determine the origin of the superior properties of DN-gels, we investigated the structure and the chain dynamics of model PAMPS/PAAm solution blends using small-angle neutron scattering and neutron spin-echo measurements. Akcasu's dynamic scattering theory for a multicomponent system is modified to include polyelectrolytes, and the resulting equation describes well the neutron spin-echo results over the entire wavevector range covered in our experiments. Parameters such as effective solvent viscosity were deduced from the measured data using the modified Akcasu equation. Both the relaxation time at large length scales (10−100 nm) and the segmental diffusion coefficient at short length scales (1−10 Å) or the effective solvent viscosity show good accordance with the macroscopic rheological behavior of the solution blends.

Introduction

Charged polymer (polyelectrolyte) systems have garnered significant interest over the past three decades due to their technological relevance and the similarities they share with biological macromolecules. The intrachain electrostatic repulsion is unique to polyelectrolytes, and their rheological behavior is thus fundamentally different from that of neutral polymers or small-molecule electrolytes. Surface and interfacial modifications, functional coatings, controlled release formulations, and superabsorbents are just a few examples of applications developed based on the unique physical properties of polyelectrolytes.[1−5] Because of their charged nature, polyelectrolytes can also electrostatically interact with neutral but polarizable components in solution. Such interactions between oppositely charged polyelectrolytes or between a polyelectrolyte and small-molecule counterions play a crucial role in a number of applications.[6−9]

We focus on the recently discovered double-network hydrogel (DN-gel) systems prepared from the combination of a cross-linked anionic polyelectrolyte, poly(2-acrylamido-2-methyl-1-propanesulfonic acid) (PAMPS), and a linear neutral polymer, polyacrylamide (PAAm).[3−5,10,11] The general scheme of combining a polyelectrolyte with a high molar mass linear polymer was shown to result in orders-of-magnitude improvement in the mechanical properties of certain cross-linked polyelectrolyte hydrogels. More specifically, the fracture strength of the PAMPS/PAAm DN-gels approaches that of tissue cartilage (∼20 MPa) at 2 mol/L PAAm concentration. Using neutron scattering, we have measured the thermodynamic interaction parameters in PAMPS/PAAm solution blends and have reached the notion that the energetically favorable interactions between the polyelectrolyte (PAMPS or PE) and the neutral polymer (PAAm or NP) are responsible for the ultimate mechanical properties of DN-gels.[12,13] In the above-mentioned work we used the multicomponent scattering theory by Benmouna and co-workers[14] to model the static structure factor of aqueous PAMPS and PAMPS/PAAm solution blends (PAMPS concentration: 0.01−0.15 mol/L) and obtained the Flory−Huggins parameters for all interaction pairs (PE−water, NP−water, PE−NP).[13] The parameter for segmental interactions between polyelectrolyte and neutral polymer was found to be much smaller than that for their respective interactions with water ($\chi_{PE-NP} \ll \chi_{PE-water} < \chi_{NP-water}$).[13] In addition, our rheological results have unraveled a composition-specific interchain association between PAMPS and PAAm.[15] To further elucidate the effect of enthalpic PAMPS−PAAm interactions on the dynamics of PAMPS chains in solutions, both small-angle neutron scattering (SANS) and neutron spin-echo (NSE) spectroscopy were applied to measure the static structure and the chain dynamics over a broad q range.

The static polymer chain conformation measured using SANS is related to the chain dynamics measured with NSE spectroscopy; i.e., as to be shown in the latter part of this work the intermediate scattering function from NSE is related to the static structure factor explicitly. In this work NSE measures the intermediate scattering function in the range from 0.056 to 0.2 $Å^{-1}$ and from 0.015 to 15 ns, respectively. NSE has been used previously to investigate the relaxation behavior of polyelectrolyte solutions.[16−20] Hayter et al. studied the dynamics of semidilute polystyrenesulfonate (PSS) in salt-free solutions,[16] and they proposed a simple model to explain the observed chain dynamics. According to their model, the diffusion coefficient ($D(q) = \tau^{-1}(q)/q^2$) of polyelectrolyte chains exhibits a q-independent behavior in the high-q region while it scales as q^{-1} in the low-q region. Nyström et al.[18] focused on the difference in relaxation behavior of PSS dissolved in solvents of different polarities and rationalized their results by following Hayter et al.'s "correlation hole" model. Kanaya et al.[19] studied the molar mass dependence of PSS dynamics in solution at a fixed polymer concentration and maintained that the transition from dilute to semidilute region occurred at a critical PSS molar mass which agreed well with their proposed phase diagram.[21] Kanaya also pointed out that while Hayter et al.'s theory highlighted the complexities of polyelectrolyte dynamics in solution, it could not quantitatively explain the NSE data in

* Corresponding author. E-mail: wenli@nist.gov.
† Polymers Division, NIST.
‡ Hokkaido University.
§ NIST Center for Neutron Research, NIST.
⊥ Present address: Cabot Corporation, 157 Concord Rd., PO Box 7001, Billerica, MA 01821-7001.

10.1021/ma802217m CCC: $40.75
Published on Web 01/22/2009

detail.[19] In general, the chain dynamics of polyelectrolytes in a multicomponent system, i.e., the subject of the current work, has not been well studied despite its relevance for many important applications.

The relaxation behavior of PAMPS chains in semidilute aqueous solutions and in blends with PAAm solutions is the focus of our current study. The dynamic structure of polyelectrolytes in multicomponent systems was quantitatively modeled following the theoretical work of Akcasu and co-workers.[22] As mentioned before, the static structure factor of polyelectrolytes is a necessary input parameter in Akcasu's theory for chain dynamics and is measured separately using SANS. The rest of this paper is arranged as follows: (i) the scattering theory proposed by Akcasu for the dynamics in multicomponent systems is discussed and modified to include a polyelectrolyte component; (ii) the sample preparation and measurement are given in the Experimental Section; (iii) the results from SANS and NSE experiments are described; (iv) the dynamic structure factor is quantitatively modeled to determine the effective solvent viscosity which governs the segmental diffusion followed by (v) discussion and conclusions.

Dynamic Scattering Theory for Multicomponent Solutions Containing Polyelectrolyte

The dynamic structure factor can be written as a simple exponential function shown in eq 1.

$$S(q,t) = S(q)\exp(-\Omega(q)t) \tag{1}$$

where $S(q)$ is the static structure factor. Following random phase approximation (RPA), $\Omega(q)$ can be expressed in terms of the static structure factor matrix $S(q)$ and the mobility matrix $M(q)$ as

$$\Omega(q) = q^2 k_B T M(q) S(q)^{-1} \tag{2}$$

where k_B is the Boltzmann constant and T is temperature. The $\Omega(q)$ matrix, in general, is not symmetric but still can be diagonalized by a similarity transformation. For a system containing polyions, counterions, and solvent (three components, hence a 2×2 matrix) we obtain two eigenvalues, Γ_s and Γ_f, for $\Omega(q)$. Inserting the eigenvalues in eq 2, we get the partial dynamic structure factor of the labeled component $S_{aa}(q,t)$ as

$$S_{aa}(q,t) = (A_{aa}e^{-\Gamma_s t} + B_{aa}e^{-\Gamma_f t})S_{aa}(q) \tag{3}$$

where the amplitudes A_{aa} and B_{aa} can be expressed in terms of $S_{ij}(q)$ and Ω_{ij}, and the relaxation frequencies Γ_s and Γ_f can be obtained by solving the quadratic equation

$$\Gamma^2 - 2\Omega_{av}\Gamma + |\Omega| = 0 \tag{4}$$

Here, $\Omega_{av} = (\Omega_{11} + \Omega_{22})/2$ and $|\Omega| = \Omega_{11}\Omega_{22} - \Omega_{12}\Omega_{21}$. The subscripts "s" and "f" refer to the "slow" and the "fast" modes, respectively. The motions of these two modes are strongly coupled at the large length scale, and they become decoupled at the small length scale. When the solute component carries charges, the electric neutrality imposes a constraint which results in a "plasmon" mode for the fast mode and its amplitude B_{aa} becomes much smaller than the slow mode.

If only one component is visible (a-species) in a multicomponent system, the initial slope (the first cumulant) Γ_{aa}, defined as $\Gamma_{aa} = -\lim_{t\to 0}[\mathrm{d}\ln S_{aa}(q,t)/\mathrm{d}t]$, can be derived from eq 3 as

$$\Gamma_{aa} = \frac{A_{aa}\Gamma_s + B_{aa}\Gamma_f}{A_{aa} + B_{aa}} \tag{5}$$

In the long time limit and in the intermediate and high-q regimes, the fast mode ("plasmon" mode) rapidly decays to zero. Hence, $S_{aa}(q,t)$ shows a single-exponential decay and Γ_{aa} can be approximated as Γ_s. Experimentally, Γ_{aa} can be easily obtained by fitting $S_{aa}(q,t)$ to a single-exponential function. To simplify the argument, we start our discussions with a ternary system, i.e., a 2×2 matrix; for a quaternary system comprising polyions, counterions, solvent, and neutral polymer the above discussions can also be extended to cover a 3×3 matrix.

On the basis of eq 2, the problem of calculating $S_{aa}(q,t)$ is reduced to the calculation of the mobility matrix $M(q)$ and the static structure matrix $S(q)$. The components $m_{ij}(q)$ of $M(q)$ can be expressed in terms of the bare mobility matrix components ($m^0_{ij}(q)$) using the RPA. In the ternary mixture of a, b, and c (solvent or matrix), we obtain the $m_{ij}(q)$ as

$$m_{ij} \approx m^0_{ij}\delta_{ij} - \frac{m^0_{ii}m^0_{jj}}{m^0_{cc} + m^0_{aa} + m^0_{bb}} \tag{6.1}$$

The bare mobility can be expressed as the sum of a free-draining part and a hydrodynamic part

$$m^0_{aa}(q) = m^0_{aa,F} + m^0_{aa,H} \tag{6.2}$$

$$m^0_{aa,F}(q) = \frac{\varphi_a}{\xi_a}, \quad m^0_{aa,H} = \frac{1}{4\pi^2\eta_s}\int \mathrm{d}k\, Z\left(\frac{k}{q}\right)S_{aa}(k) \tag{6.3}$$

$$Z\left(\frac{k}{q}\right) = \frac{q^2 + k^2}{2qk}\ln\frac{|q+k|}{|q-k|} - 1 \tag{6.4}$$

where φ_a is the volume fraction of species a, ξ_a is the monomeric friction coefficient, and η_s is the viscosity of solvent. Following the Stokes–Einstein relation, the left term in eq 6.3 can be rewritten as $m^0_{aa,F} = \varphi_a/6\pi\eta_s a$ (a: monomer size). m^0_{cc} in eq 6.1 is just the mobility of solvent. By treating the solvent molecules as noninteracting fictitious monomers and using the dynamic response theory, m^0_{cc} can be expressed as $n_s D_s/k_B T$ where n_s is the number density and D_s is the diffusion coefficient of solvent, respectively. Given that the diffusion of solvent molecules is much faster than the other components in the system, the second term in eq 6.1 becomes negligible. In this study the volume fraction of the solvent is larger than 0.9, and it follows that $m_{ii} \sim m^0_{ii}$.

In eq 2, each parameter of the first cumulant matrix can be obtained only when all parameters of the static structure matrix are known. However, when only the labeled species a is visible the following equation becomes valid:

$$\Gamma_{aa}(q) = q^2 k_B T m_{aa}(q) S_{aa}(q)^{-1} \tag{7}$$

It is important to note that Γ_{aa} is not the component of the first cumulant matrix Ω_{ij}.

The arguments above are applicable to multicomponent polymer mixtures in general, including polyelectrolyte solutions.[23,24] The presence of polyelectrolytes in the multicomponent system and their unique properties necessitate further considerations. The dynamic scattering function for polyelectrolyte solutions has been theoretically investigated for several decades.[16,25–30] In summary, most developments[25–30] have been for weakly charged (flexible) polyelectrolyte solutions, and the left part of eq 6.3 (the free-draining contribution) by itself is a reasonable approximation for the bare mobility. For strongly charged polyelectrolyte solutions as in this work the rigidity of polyelectrolyte affects the free-draining term in the length scale probed by NSE and is included in the theoretical approach developed by Hayter et al.[16] In their model, the hydrodynamic

contribution of the mobility is not considered ($m_{aa}(q) = m_{aa,F}$). Their expression of mobility in the wavevector range, $q > l_p^{-1}$ (l_p: persistence length) is

$$m_{aa}(q) = \frac{m_0}{q l_p} \tag{8}$$

In eq 8, the factor $(ql_p)^{-1}$ was introduced to accommodate the rigid nature of strongly charged polyelectrolyte chains. At small q, this force acts over wavelengths larger than the chain length and the chain responds as a whole, while at large q, the force fields are smaller than the chain dimension; hence, the individual portion of chain can be considered to feel the force in the opposite direction.[31] As a result, the net response decreases as q increases. Pincus has derived this factor for a polymer chain constrained in a tube (reptation model) and is experiencing a spatially periodic longitudinal force.[32] By replacing the tube length (the entanglement length) with the persistence length, the same argument can be applied to rigid polyelectrolyte and to obtain the factor (Onsager transport coefficient) as $(1 - \exp(-q^2 l_p^2))/q^2 l_p^2$. To complete the free-draining part, we need to estimate the prefactor m_0 in eq 8. In the limit of small q (the hydrodynamic interaction is assumed to be completely screened at this limit), Pincus' factor reduces to unity and the effective diffusion coefficient D can be written as

$$D = \frac{k_B T}{N_{PE} \xi_{PE}} \tag{9}$$

where N_{PE} is the number of monomers in a PAMPS blob and ξ_{PE} is the monomeric friction coefficient of PAMPS. Following the Stokes−Einstein relation, however, the diffusion coefficient can also be expressed as

$$D = \frac{k_B T}{6\pi\eta_s R_H} \tag{10}$$

where R_H is the hydrodynamic radius of a PAMPS blob and η_s is the effective solvent viscosity experienced by PAMPS while the combination of water and PAAm is considered as the solvent. The monomeric friction coefficient ξ_{PE} can thus be obtained from eqs 9 and 10 as

$$\xi_{PE} = \frac{6\pi\eta_s R_H}{N_{PE}} \tag{11}$$

If we assume $R_H \sim$ blob size, N_{PE} can be replaced by const$\cdot R_H^2$ from the scaling theory.[33] Following these arguments, eq 7 can now be rewritten as

$$\Gamma_{aa}(q) = q^2 k_B T \left(\frac{\text{const} \cdot R_H \varphi_a}{6\pi\eta_s} \frac{1 - \exp(-q^2 l_p^2)}{q^2 l_p^2} + \frac{1}{4\pi^2 \eta_s} \int \mathrm{d}k \, Z\left(\frac{k}{q}\right) S_{aa}(k) \right) S_{aa}(q)^{-1} \tag{12}$$

The above equation relates a dynamic quantity to a static structure factor and will be used extensively in the rest of this article to fit the NSE data. With this equation the q-dependent relaxation time, i.e., effective diffusion coefficient ($D_{eff}(q) = \Gamma(q)/q^2$) can be calculated directly from experimentally observed static structure factor $S_{aa}(q)$, effective solvent viscosity η_s, and the blob size R_H. All the effects originating from the interchain interactions between different components, i.e., polyelectrolyte−solvent, neutral polymer−solvent, and polyelectrolyte−neutral polymer, are implicitly included in the static structure factor $S_{aa}(q)$ and the effective solvent viscosity η_s. The former can be measured directly using SANS while the latter will be deduced from the NSE data using eq 12.

Table 1. Compositions (in Volume Fraction (φ)) of the 0.5 mol/L PAMPS and PAMPS/PAAm Solution Blends Used in This Study[a]

sample (PE:NP)	PE concn [mol/L]	φ_{PE}	φ_{NP}	φ_S
1:0	0.5	0.0858	0	0.914
3:1	0.375	0.0644	0.0082	0.927
1:3	0.125	0.0215	0.0245	0.954
1:7	0.0625	0.0107	0.0287	0.961
1:15	0.031 25	0.0053	0.0307	0.964

[a] Subscript PE, NP, and S stand for PAMPS, PAAm, and water, respectively. The ratio listed in the first column designates the monomer molar ratio of PAMPS to PAAm.

Experimental Section

Starting Materials.[34] 2-Acrylamido-2-methyl-1-propanesulfonic acid (AMPS) (monomer; TCI America) and 2-oxoglutaric acid (initiator, Polysciences, Inc.) were used as received. Deuterium-labeled acrylamide monomer (d_3AAm) free of inhibitor was obtained from Cambridge Isotope Laboratories, Inc., and was used as received. Deuterated water was used as received from Aldrich Chemical Co.

Polymer Synthesis. Pure PAMPS and d_3PAAm solutions were prepared at a concentration of 0.5 mol/L by UV-initiated free-radical polymerization of their monomers in deuterated water, codissolved with 0.1 and 0.01 mol % 2-oxoglutaric acid, respectively. Solution phase blends were prepared by mixing linear polymer solutions of PAMPS and d_3PAAm at various volume ratios, as shown in Table 1. The mixtures were homogenized by continuous stirring for 4 days prior to the neutron scattering and neutron spin-echo spectroscopy measurements.

Small-Angle Neutron Scattering Measurements.[35] Small-angle neutron scattering measurements were performed using the 30 m NG7 beamline at the NIST Center for Neutron Research (NCNR).[36] Scattering data were acquired at sample-to-detector distances 1 and 5 m using a neutron wavelength of $\lambda = 8.09$ Å and a wavelength spread, $\Delta\lambda/\lambda = 0.11$. This provides a q range of 0.0085 Å$^{-1} \le q \le 0.15$ Å^{-1}. SANS data were reduced to absolute intensity by subtracting contributions from the instrument background and incoherent scattering from the sample and correcting for variations in the detector sensitivity.[37] The solvent is a mixture of deuterated and protonated water, and its neutron scattering length b_S matches that of d_3PAAm. The neutron scattering intensities, for both SANS and NSE, were thus originated from the contrast defined as $b_{PE} - b_S$ where b_{PE} is the neutron scattering length of PAMPS, i.e., the polyelectrolyte. To facilitate data comparison among samples with different concentrations of PAMPS, the scattering intensity in its absolute unit (cm^{-1}) was further normalized by the neutron contrast factor, $(b_{PE} - b_S)^2$, and the volume fraction factor, $\varphi_{PE}(1 - \varphi_{PE})$, as described previously.[12,13] φ_{PE} stands for the volume fraction of PAMPS in the sample.

Neutron Spin-Echo Measurements. Neutron spin-echo spectroscopy measurements were conducted on the NG5-NSE beamline at NCNR.[38,39] The incident neutron beam of 6 Å wavelength was mechanically selected with a 20% full width at half-maximum wavelength distribution. The measured wavevector (q) and time ranges were from 0.056 to 0.2 Å^{-1} and from 0.015 to 15 ns, respectively. The samples were contained in a standard sample cell with quartz windows of 1 mm thickness and a path length of 4 mm. All the samples were measured at a constant temperature of 25 °C. The spectroscopy data from neutron spin-echo measurements was reduced and analyzed using the DAVE software package.[40] All the samples had their neutron scattering contrast matched between the water and d_3PAAm, just as for the case of SANS measurements.

Results and Discussion

Small-Angle Neutron Scattering. Figure 1a,b shows the small-angle neutron scattering (SANS) intensities from aqueous

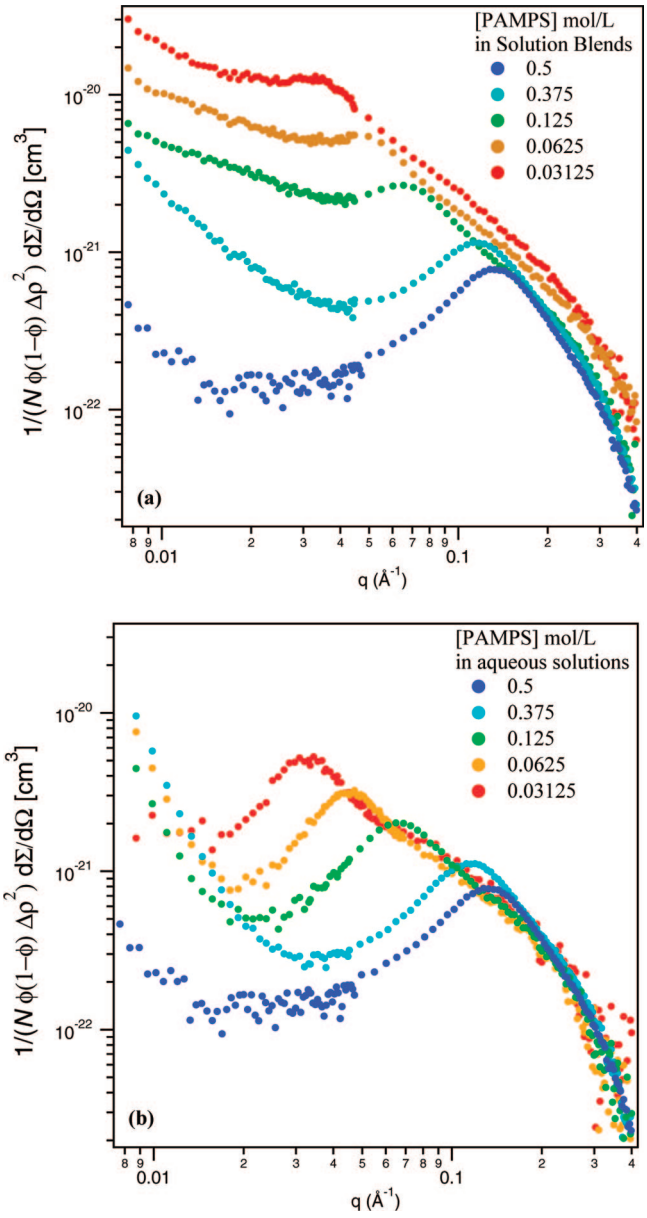

Figure 1. SANS spectra of (a) aqueous PAMPS/PAAm solution blends and (b) pure PAMPS solutions at PAMPS concentrations given in the legend.

solutions of PAMPS and its blends with d_3PAAm solutions at various molar ratios. In the blend solutions, the total polymer concentration is kept constant (0.5 mol/L) while the molar ratio between PAMPS and PAAm is varied. Both the pure PAMPS solutions and its blends with d_3PAAm exhibit a maximum in the normalized neutron scattering intensity typical of scattering from polyelectrolyte systems. The wave vector corresponding to the intensity maximum (q^*) is related to the Debye screening length (κ^{-1}) which depends on polyelectrolyte concentration by following a well-established scaling relationship $\kappa^{-1} \sim c^{-0.5}$, where c is the molar concentration of polyelectrolyte. We notice that the q^* of PAMPS/d_3PAAm solution blends is the same as that of corresponding pure PAMPS solutions and scales with polyelectrolyte concentration as $c^{-0.51\pm0.04}$. The scattering profiles from PAMPS/d_3PAAm solution blends, however, are markedly different from those of pure PAMPS solutions, especially at the low-q region ($q < q^*$). Scattering results from pure PAMPS solutions exhibit a well-defined maximum for all PAMPS concentrations whereas those from PAMPS/d_3PAAm solution blends exhibit an intensity maximum that is smeared at $q < q^*$,

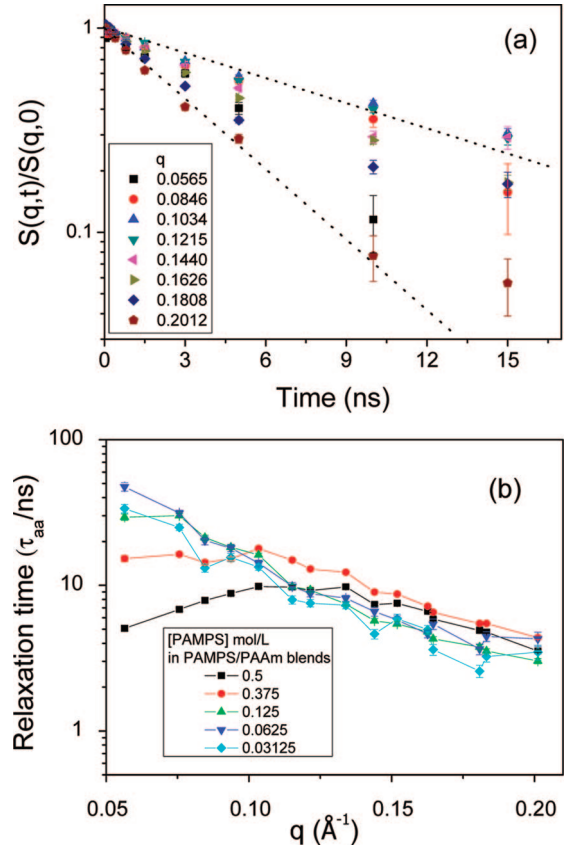

Figure 2. (a) Intermediate scattering function of PAMPS in 0.5 mol/L PAMPS solution. Dotted lines are drawn as a guide for the eye. (b) q-dependent relaxation time of the PAMPS solution and PAMPS/PAAm solution blends.

especially for polyelectrolyte concentrations less than 0.125 mol/L. The solution blends exhibit a weaker upturn ($I_{11} \sim q^{-2}$) in forward scattering intensity than the pure PAMPS solutions ($I_{11} \sim q^{-3}$) as q approaches zero, which qualitatively corresponds to a lower zero angle scattering intensity. This observation is consistent with our previous results in which the addition of PAAm was found to suppress imhomogeneities in the pure PAMPS solutions. The above-mentioned SANS results have been analyzed quantitatively, and a near-zero Flory−Huggins interaction parameter between PAMPS and PAAm was obtained.[13] This low value of interaction parameter is reminiscent of the good compatibility between these two polymers. Similar SANS results in aqueous PAMPS solution have been reported for the case of poly(styrenesulfonate) (PSS) solutions.[46,47] The authors claimed that this power law behavior is a manifestation of the globular domain formation among the hydrophobic PSS backbone, and this notion was further supported using light scattering.[47] The backbone of PAMPS is also hydrophobic as PSS; the domain formation in aqueous PAMPS solutions cannot be ruled out in this case. In the case of PAMPS/PAAm solution blends, especially at PAMPS concentrations ≤0.125 mol/L (corresponding to high PAAm concentration), the intensities at very low q decreased with the power law of $\sim q^{-2}$ (Figure 1a). Ermi et al. observed the power law of −2 in the SANS experiments of poly(*N*-methyl-2-vinylpyridinium chloride) solutions (hydrophilic backbone) and claimed this to be the result of formation of fractal objects in the solutions.[48]

Neutron Spin-Echo Spectroscopy. *i. Aqueous PAMPS Solutions.* The intermediate scattering functions of 0.5 mol/L aqueous PAMPS solutions are given in Figure 2a. The results can be modeled as a single-exponential decay over the entire q range and the relaxation time ($\tau_{aa}(q)$) defined in $S_{aa}(q,t)/S_{aa}(q,0)$

Table 2. Best Fit Parameters Used in Eq 12 To Describe the Chain Dynamics of PAMPS in Pure PAMPS Solution and in PAMPS/PAAm Solution Blends[a]

samples (PE:NP)	η_s ($\times 10^3$ Pa·s)	const·R_H
pure PE 0.5 M	5.32	9.1
3:1	5.83	6.8
1:3	6.16	38.3
1:7	7.14	81.3
1:15	5.77	186.5

[a] The standard uncertainty in estimation of each parameter from data fitting is about 0.1%.

$= A \exp(-t/\tau_{aa}(q))$ was obtained. In the cases of PAMPS/PAAm blend solutions a single-exponential decaying intermediate function was also observed. The q-dependent relaxation times of both the PAMPS solution and solution blends are given in Figure 2b together with the q-dependent effective diffusion coefficient $D_{aa,\mathrm{eff}}(q) = \tau_{aa}^{-1}(q)/q^2 = \Gamma_{aa}(q)/q^2$ based on Hayter et al.'s definition.[16] These experimental results of $\Gamma_{aa}(q)/q^2$ will be analyzed using eq 12 with the following input parameters. The partial static structure factor of PAMPS ($S_{aa}(q)$) was obtained from the SANS measurements (Figure 1a), and the persistence length (l_p) was calculated from the relation of $l_p = I^{-0.5}$ (I: ionic strength).[41] The monomer size a of PAMPS is estimated by the density obtained from pycnometry (0.575 cm^3/g).[42] η_s and const·R_H are the only two fitting parameters for eq 12. To fit the experimental data, we employed the Levenberg−Marquardt nonlinear fitting method.[43]

The best fitted values for η_s and const·R_H are listed in Table 2. According to the definition of hydrodynamic interaction, η_s is the viscosity of solvent, and in the present case of polymer solution blends it is the effective viscosity experienced by PAMPS chains via the interactions with both water molecules and PAAm chains. The presence of polymer solutes will definitely affect the solvent mobility, and the viscosity of the effective medium has to be different from that of neat solvents (1.0×10^{-3} Pa·s for water at 20 °C).[44] Therefore, this effective solvent viscosity is chosen as one of the fitting parameters. In Figure 3a, we show the q-dependent effective diffusion coefficient of PAMPS chains in 0.5 mol/L pure PAMPS solution. As the previous neutron spin-echo studies of semidilute polyelectrolyte solutions[16−19] have shown, the diffusion coefficient shows a sharp decrease with q at the low-q region ($q < q^*$) while it stays nearly constant or slightly increases at high q ($q > q^*$).

ii. PAMPS/PAAm Solution Blends. In the previous publication[12] we have suggested that interchain PAMPS/PAAm association in aqueous solutions is responsible for the observed viscosity enhancement; a maximum in viscosity near the volume ratio (PAMPS:PAAm) of 1:7 was observed. The ratio over which the viscosity maximum occurred was found to be independent of total polymer concentration but coincided with the composition range over which the DN-gels exhibit their optimal mechanical properties. The exact mechanism of PAMPS/PAAm association is not known yet. However, recent density functional theory calculations indicate that the intermolecular energy between PAMPS and PAAm reaches a minimum via hydrogen bonding at this composition.[12] The purpose of this NSE study is to determine whether this compositional dependent viscosity enhancement manifests itself in the chain dynamics over a broad q range covered by NSE measurements.

In all the solution blend samples, the intermediate scattering functions show a single-exponential decay over the entire q range as the pure PAMPS solutions. This indicates that the presence of neutral polymer did not induce an anomalous diffusion behavior of polyelectrolyte chains despite the marked change in the relaxation time of polyelectrolyte chains. As shown in Figure 2b, the q-dependent relaxation time spectra of

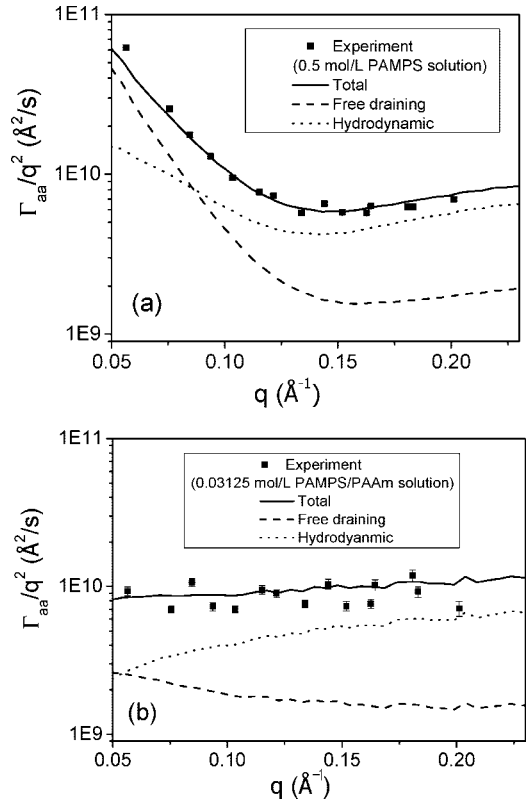

Figure 3. (a) q-dependent effective diffusion coefficient of the 0.5 mol/L PAMPS solution and the fit using eq 12. (b) q-dependent effective diffusion coefficient and the fit using eq 12 of the PAMPS/PAAm solution blend containing 0.031 25 mol/L PAMPS.

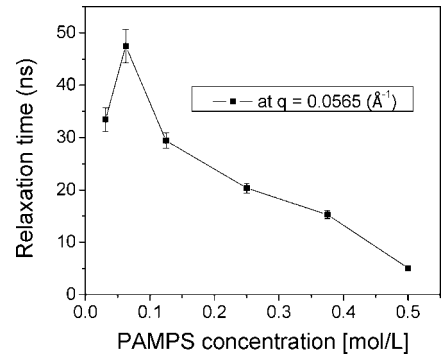

Figure 4. Relaxation time measured at $q = 0.0565$ Å^{-1} of PAMPS chain in PAMPS/PAAm solution blends of different compositions. The total polymer concentration was kept at 0.5 mol/L for all the samples.

various compositions seem to follow the static structure factors (Figure 1a). However, at the lowest accessible q of 0.0565 Å^{-1} the 1:7 PAMPS/PAAm solution blend (0.0625 mol/L PAMPS) has a maximum relaxation time (Figure 4), and this is in good agreement with the viscosity results.[12] In Figure 5a, the q-dependent diffusion coefficients of PAMPS chains in PAMPS/PAAm solution blends are given together with the fits using eq 12. With two fitting parameters, η_s and const·R_H, eq 12 is adequate to model all the experimental results. The results of the best fit of these two parameters are listed in Table 2. A detailed example of modeling the experimental data of the 0.5 mol/L pure PAMPS solution and the 1:15 PAMPS/PAAm solution blend (0.031 25 mol/L PAMPS) using eq 12 is given in parts a and b of Figure 3, respectively. The best fit values of the effective solvent viscosity, η_s, are given in Figure 5b. The value of the 1:7 sample is unusually high compared to the other

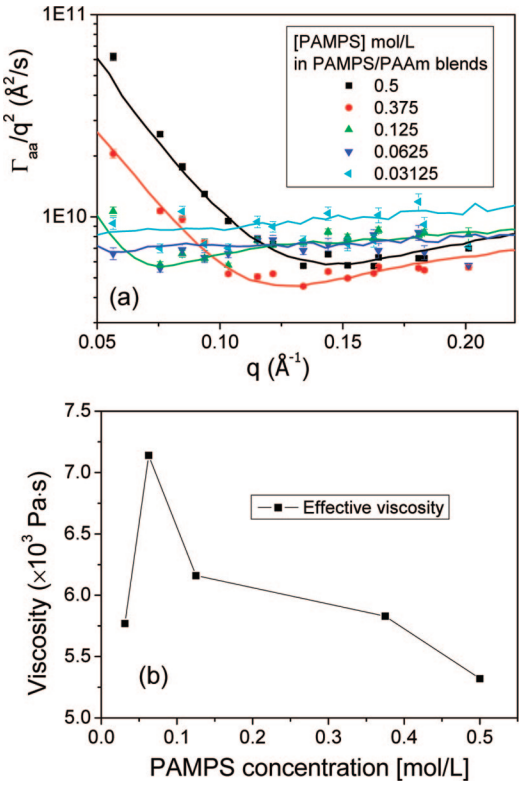

Figure 5. (a) q-dependent effective diffusion coefficient of PAMPS chain in aqueous solution and in PAMPS/PAAm solution blends. The solid lines represent the best fit using eq 12. (b) Best fit value of the effective solvent viscosity of PAMPS/PAAm solution blends of different compositions.

samples. The solvent viscosity η_s can be interpreted as the "effective medium viscosity" in which the PAMPS segments are diffusing, and it is also one of the microscopic (molecular level) measures of system properties. The other fitting parameter, const·R_H, satisfies the relationship (const·$R_H \sim c^{-1.09}$) as expected from the scaling arguments of polyelectrolyte solutions.[33,45] This observation implies that $R_H \sim \xi$ (blob size) of PAMPS is a reasonable approximation. In addition, it also indicates that the presence of neutral polymers does not affect this simple scaling relation. From the two scaling relations, i.e., $\kappa^{-1} \sim c^{-0.5}$ and R_H (or ξ) $\sim c^{-1}$, the relation ($\xi \sim \kappa^{-2}$) between the blob size and the Debye screening length is reached. This relation was proposed and used in our previous study of the static structures of linear PAMPS/PAAm solution blends.[13]

Conclusions

As demonstrated by eq 12, the first cumulant or the effective diffusivity of solution blends can be treated as a sum of two parts—a free-draining part and a hydrodynamic one—whereas in simple Rouse dynamics only the free-draining part is considered. As demonstrated in this work that the hydrodynamic contribution cannot be ignored at short length scales, for example, in a relatively concentrated (0.5 mol/L) pure PAMPS solution (Figure 3a) the free-draining contribution is dominant in the low-q region whereas the hydrodynamic contribution takes over in the high-q region. As shown in Figure 3b, the hydrodynamic contribution dominates across the entire q range covered by the present NSE measurements for PAMPS/PAAm solution blend with 0.031 25 mol/L PAMPS concentration.

Our analysis for polyelectrolyte solution dynamics has some obvious limitations; first of all, the screening of hydrodynamic interaction is not considered in order to simplify the argument. Several treatments, such as screened Oseen tensor,[49] renormalization of q-dependent viscosity,[50] or two-part (in/out of hydrodynamic blob) integration method,[51,52] can be applied to include the screening effect but would require an additional parameter to model the experimental data.

The effective solvent viscosity and the relaxation time of the 1:7 PAMPS/PAAm blend solution at large length scale are clearly different from those at other compositions. However, this difference is not as prominent as the rheological results, e.g., the effective solvent viscosity η_s increases by ~20% whereas the zero shear viscosity of the solution increases by an order of magnitude.

In summary, SANS and NSE experiments were performed on the model solution blends containing linear PAMPS and PAAm chains to investigate the molecular origin of strength of DN-gels prepared from PAMPS and PAAm. The static structure of PAMPS chains revealed by SANS exhibits a marked change in the low-q region with the addition of PAAm. NSE results revealed anomalous diffusion behavior of PAMPS chains in PAMPS/PAAm solution blend at a 1:7 PAMPS/PAAm molar ratio; a long relaxation time at length scales on the order of 50−100 nm and a high effective medium viscosity. This is also the only composition at which the solution blends exhibit a maximum in zero shear viscosity, and concurrently the DN-gels exhibit their optimal mechanical properties. The neutron spin-echo results were analyzed by modifying Akcasu's dynamic scattering theory to include polyelectrolyte interactions. With the modified Akcasu equation, the static structure factors measured with SANS and two adjustable parameters, η_s and R_H, were used to describe the dynamics of PAMPS chain in PAAm solution blends. The best fit values of hydrodynamic radius closely follow a simple scaling relation known for aqueous polyelectrolyte solutions, and the fitted value of the effective solvent viscosity supports the notion that the extent of PAMPS/PAAm association depends on composition and reaches a maximum near 1:7 PAMPS/PAAm molar ratio.

Acknowledgment. All the neutron measurements were conducted at the NIST Center for Neutron Research; some of the neutron facilities used are supported in part by the National Science Foundation under Agreement DMR-0454672. J.P.G. acknowledges a Grant-in-Aid for fundamental research and a Grant-in-Aid for Creative Scientific Research from the Ministry of Education, Science, Sports, and Culture of Japan.

References and Notes

(1) Hara, M. *Polyelectrolyte, Science and Technology*; Marcel Dekker: New York, 1993.
(2) Harland, R. S., Prud'homme, R. K., Eds.; *Polyelectrolyte Gels: Properties, Preparation, and Applications*; ACS Symposium Series 480; American Chemical Society: Washington, DC, 1998.
(3) Gong, J. P.; Katsuyama, Y.; Kurokawa, T.; Osada, Y. *Adv. Mater.* **2003**, *15*, 1155.
(4) Kaneko, D.; Tada, T.; Kurokawa, T.; Osada, Y. *Adv. Mater.* **2005**, *17*, 535.
(5) Nakayama, A.; Kakugo, A.; Gong, J. P.; Osada, Y.; Takai, M.; Erata, T. *Adv. Funct. Mater.* **2004**, *14*, 1124.
(6) Decher, G. *Science* **1997**, *277*, 1232.
(7) Decher, G.; Hong, J. D.; Schmitt, J. *Thin Solid Films* **1992**, *210*, 831.
(8) Lvov, Y.; Ariga, K.; Ichinose, I.; Kunitake, T. *J. Am. Chem. Soc.* **1995**, *117*, 6117.
(9) Han, S. B.; Briseno, A. L.; Shi, X. Y.; Mah, D. A.; Zhou, F. M. *J. Phys. Chem. B* **2002**, *106*, 6465.
(10) Yasuda, K.; Gong, J. P.; Katsuyama, Y.; Nakayama, A.; Tanabe, Y.; Kondo, E. *Biomaterials* **2005**, *26*, 4468.
(11) Webber, R. E.; Creton, C.; Brown, H. R.; Gong, J. P. *Macromolecules* **2007**, *40*, 2919.
(12) Tominaga, T.; Tirumala, V. R.; Lin, E. K.; Gong, J. P.; Furukawa, H.; Osada, Y.; Wu, W.-L. *Polymer* **2007**, *48*, 7449.
(13) Tominaga, T.; Tirumala, V. R.; Lee, S.; Lin, E. K.; Gong, J. P.; Wu, W.-L. *J. Phys. Chem. B* **2008**, *112*, 3903.

(14) Benmouna, M.; Vilgis, T. A.; Hakem, F.; Negadi, A. *Macromolecules* **1991**, *24*, 6418.
(15) Tirumala, V. R.; Tominaga, T.; Lee, S.; Butler, P. D.; Lin, E. K.; Gong, J. P.; Wu, W.-L. *J. Phys. Chem. B* **2008**, *112*, 8024.
(16) Hayter, J.; Jannink, G.; Brochard-Wyart, F.; de Gennes, P. G. *J. Phys., Lett.* **1980**, *41*, L-451.
(17) Nallet, F.; Jannink, G.; Hayter, J. B.; Oberthür, R.; Picot, C. *J. Phys. (Paris)* **1983**, *44*, 87.
(18) Nyström, B.; Roots, J.; Higgins, J. S.; Gabrys, B.; Peiffer, D. G.; Mezei, F.; Sarkissian, B. *J. Polym. Sci., Part C: Polym. Lett.* **1986**, *24*, 273.
(19) Kanaya, T.; Kaji, K.; Kitamaru, R.; Higgins, J. S.; Farago, B. *Macromolecules* **1989**, *22*, 1356.
(20) Prabhu, V. M.; Amis, E. J.; Bossev, D. P.; Rosov, N. *J. Chem. Phys.* **2005**, *121*, 4424.
(21) Kaji, K.; Urakawa, H.; Kanaya, T.; Kitamaru, R. *J. Phys. (Paris)* **1988**, *49*, 993.
(22) Akcasu, A. Z. In *Dynamic Light Scattering. The Method and Some Applications*; Brown, W. Ed.; Oxford University Press: London, 1992, and references therein.
(23) Benmouna, M.; Duval, M.; Strazielle, C.; Hakem, F-.I. *Acta Polym.* **1996**, *47*, 29.
(24) Montes, H.; Monkenbusch, M.; Willner, L.; Rathgeber, S.; Fetters, L.; Richter, D. *J. Chem. Phys.* **1999**, *110*, 10188.
(25) Akcasu, A. Z.; Benmouna, M.; Hammouda, B. *J. Chem. Phys.* **1984**, *80*, 2762.
(26) Ajdari, A.; Leibler, L.; Joanny, J.-F. *J. Chem. Phys.* **1991**, *95*, 4580.
(27) Genz, U.; Benmouna, M.; Klein, R. *Macromolecules* **1991**, *24*, 6413.
(28) Benmouna, M.; Vilgis, T. A.; Hakem, F. *Macromolecules* **1992**, *25*, 1144.
(29) Borsali, R. *Macromol. Chem. Phys.* **1996**, *197*, 3947.
(30) Siciliano, A.; Perico, A. *Macromolecules* **1996**, *29*, 2068.
(31) Sivaniah, E.; Jones, R. A. L.; Sferrazza, M. *Phys. Rev. E* **2003**, *67*, 052801.
(32) Pincus, P. *J. Chem. Phys.* **1981**, *75*, 1996.
(33) Dobrynin, A. V.; Rubinstein, M. *Prog. Polym. Sci.* **2005**, *30*, 1049.
(34) Certain equipment, instruments or materials are identified in this paper in order to adequately specify the experimental details. Such identification does not imply recommendation by the National Institute of Standards and Technology nor does it imply the materials are necessarily the best available for the purpose.
(35) The uncertainty in measured neutron scattering data is less than the size of the markers used unless explicitly shown using error bars.
(36) Glinka, C. J.; Barker, J. G.; Hammouda, B.; Krueger, S.; Moyer, J. J.; Orts, W. J. *J. Appl. Crystallogr.* **1998**, *31*, 430.
(37) Kline, S. R. *J. Appl. Crystallogr.* **2006**, *39*, 895.
(38) Monkenbusch, M.; Schätzler, R.; Richter, D. *Nucl. Instrum. Methods Phys. Res., Sect. A* **1997**, *399*, 301.
(39) Rosov, N.; Rathgeber, S.; Monkenbusch, M. Neutron Spin Echo Spectroscopy at the NIST Center for Neutron Research In *Scattering from Polymers: Characterization by X-rays, Neutrons, and Light*; Cebe, P., Hsaio, B. S., Lohse, D. J., Eds.; American Chemical Society: Washington, DC, 2000; ACS Symp. Ser. *739*, p 103.
(40) http://www.ncnr.nist.gov/dave.
(41) Tricot, M. *Macromolecules* **1984**, *17*, 1698.
(42) Zhou, Z.; Childs, R. F.; Mika, A. M. *J. Membr. Sci.* **2005**, *254*, 89.
(43) Press, S. H.; Teukolsky, S. A.; Vetterling, W. T.; Flannery, B. P. *Numerical Recipes, The Art of Scientific Computing*, 3rd ed.; Cambridge University Press: New York, 2007.
(44) Lodge, T. P. *J. Phys. Chem.* **1993**, *97*, 1480.
(45) Odijk, T. *Macromolecules* **1979**, *12*, 688.
(46) Matsuoka, H.; Schwahn, D.; Ise, N. In *Macro-Ion Characterization: From Dilute Solutions to Complex Fluids*; Schmitz, K. S., Ed.; ACS Symposium Series 548; American Chemical Society: Washington, DC, 1993; Chapter 27.
(47) Zhang, Y.; Douglas, J. F.; Ermi, B. D.; Amis, E. J. *J. Chem. Phys.* **2001**, *114*, 3299.
(48) Ermi, B. D.; Amis, E. J. *Macromolecules* **1998**, *31*, 7378.
(49) Borsali, R.; Vilgis, T. A.; Benmouna, M. *J. Phys. II* **1993**, *3*, 625.
(50) Richter, D.; Ewen, B.; Binder, K. *J. Phys. Chem.* **1984**, *88*, 6618.
(51) Roby, F.; Joanny, J. F. *Macromolecules* **1992**, *25*, 4612.
(52) Hammouda, B. *Macromolecules* **1993**, *26*, 4800.

MA802217M